Journal of Intelligent Systems and Internet of Things
Vol. 17, No. 01, PP. 196-207, 2025
DOI: https://doi.org/10.54216/JISIoT.170114

Hybrid Compressive Sensing based Secure Medical Image Compression and Reconstruction in Telemedicine Application

Shilpa A. N.[1,2,3,*], Santosh Kumar G.[4], Veena C. S.[5]

[1]Department of Electronics Communication and Engineering, Research Scholar, East West College of Engineering, India

[2]Visvesvaraya Technological University-Research Center, Bengaluru-560064, Karnataka, India

[3]Department of Electronics Communication and Engineering, Senior Scale Lecturer, Government Polytechnic Chamarajanagar-571313, Karnataka, India

[4]Director, East West College of Engineering, VTU-RC, Bengaluru-560064, Karnataka, India

[5]Department of Electronics Communication and Engineering, Professor, Presidency University, Bengaluru-560064, India

Emails: shilpa.an@gmail.com; santhoshkumarg@ewce.edu.in; veena.cs@presidencyuniversity.in

Abstract

The transmission of complex medical images in telemedicine applications poses significant challenges. An effective hybrid compressed sensing and encryption framework is proposed for enabling efficient MRI compression and secure transmission in telemedicine applications. Firstly, a fuzzy-logic-based image enhancement is pressed. Then an optimized chaotic sequence generation scheme is formulated based on image characteristics to achieve compression robustness and security of the compression process. In addition, the proposed framework uses a lightweight public key encryption method to speed up encryption and decryption time. Our experimental results demonstrate the effectiveness of the proposed system on various metrics, including PSNR, SSIM, correlation coefficient, and processing time. The system consistently achieved high SSIM scores (0.96 to 1.0) and maintained low algorithm processing time, validating its efficiency in high-quality reconstruction.

Received: January 22, 2025 Revised: March 01, 2025 Accepted: April 09, 2025

Keywords: Fuzzy Logic; Compressive Sensing; Telemedicine; Hybrid Compression

1. Introduction

Telemedicine has revolutionized healthcare by enabling remote diagnosis and treatment via the transmission of medical information, which is effective for patients in rural locations or with poor access to specialist care [1-3]. Hospitals generate a high volume of images per patient, and managing such data presents challenges for storage systems, especially since retaining medical records is mandatory. Additionally, transmitting large images over wireless networks demands high bandwidth, which is problematic in rural areas where network issues hinder data transmission and healthcare delivery [4-5]. Moreover, medical images transmitted over wireless channels enhance telehealth accessibility but expose them to cyber threats and security attacks [6]. Furthermore, not all telemedicine platforms encrypt medical images during transmission, making them vulnerable to unauthorized access, identity theft, ransom, and even sale on the dark web, leading to misdiagnosis, treatment errors, and even physical harm to patients [7]. Therefore, in a telemedicine environment, it is very important to maintain the confidentiality and integrity of medical images during transmission [8].

In exploring state-of-the-art solutions, it becomes apparent that numerous researchers have developed methods for medical image compression and encryption. However, most studies focus on either compression or encryption individually and very few have integrated both together. Apart from this, the research studies on combining

compression and encryption using compressed or compressive sensing (CS) is very less due to its underlying complexity and relatively early stage of development. A research work carried out by Anusuya et al. [9] addressed 3D MRI image compression using 2D-stationary wavelet transform, optimized embedded block and arithmetic coding for achieving better lossless compression and transmission speed. Sheeja et al. [10] presented transmitting large medical images in wireless sensor networks for disaster telemedicine using optimized network clustering, fuzzy logic, and genetic algorithms for data relay. This includes compression and maintaining clinical detail via multiple description encoding. However, sensor node use in disaster scenarios raises privacy and security concerns. Kaur and Wasson [11] suggested ROI-aware compression combining fractal lossless coding for non-ROI and weighted context tree compression for ROI. Kumar et al. [12] used adaptive vector quantization with simulated annealing for codebook optimization. The researchers in [13] used wavelet transform and Huffman coding with chaos theory for ECG compression and encryption but face issues with high-frequency components. Suhail and Sankar [14] integrated logistic-map encryption with autoencoder compression. Baranwal et al. [15] proposed chaotic maps with Huffman encoding, and reconstruction via YOLO learning network.

The above-discussed approaches offer storage and transmission cost reduction. However, they are not suitable for telemedicine due to high computational needs and complex real-time processing. Sharing key attributes for decryption and reconstruction also needs secure transmission, which is not well addressed in literature. Recently, CS has gained attention for image compression and encryption. Unlike traditional methods sampling at the Nyquist rate, CS extracts signal information from fewer measurements [16-17]. Zhou et al. [18] and Chai et al. [19] studied the CS framework and highlighted its strengths and limitations in medical imaging. Brahim et al. [20] proposed a CS-based lightweight encryption framework, but decryption needs the same key used in encryption. Lakshminarayana and Sarvagya [21] introduced a hybrid method applying lossless compression to RoI and CS to non-RoI areas, balancing compression quality and processing time. The work done by Zhu et al. [22] used CS with a logistic map for compression and encryption, which is only suitable for controlled environments, not healthcare contexts. Quan et al. [23] applied a CS framework using generative adversarial networks (GAN) for MRI reconstruction, which found to be effective but challenged by GAN training stability and computation load. Monika and Dhanalakshmi [24], adopted an adaptive block CS approach for various medical images and to achieve a high compression ratio coefficient mixed thresholding scheme is further integrated within CS. The study of Vivekanand et al. [25] applied CS for spectrum allocation in cognitive radio telemedicine, but may face real-time efficiency issues.

The problem description

It can be seen that in the literature, many compression-based methods have been proposed to reduce the file size for faster transmission. However, these methods often depend on complex compression algorithms [26-29]. In terms of data security, hybrid encryption and various customized encryption methods are used to secure medical data during transmission. While these techniques provide strong encryption, they are primarily suited for smaller medical data like clinical notes and electronic health records. Applying them to large-size data like MRI scans is resource-intensive and may not guard against advanced cyber threats. Complex encryption also slows down transmission, especially in limited bandwidth regions. CS-based research showed efficient compression and encryption with less computational load. However, CS techniques introduce some error, and reconstructing high-resolution images from compressed data poses challenges [30-32]. During compression, image information is concentrated into fewer measurements, which may unintentionally highlight details not visible in the original image. For example, pathological or anatomical features may appear more visible in compressed data. Hence, a measurement matrix must be robust and randomized to ensure reliability-aware reconstruction.

The proposed scheme

This paper presents an effective numerical algorithm and computational scheme to address the above-identified research problem. The proposed design adopts an analytical approach, and introduces a fuzzy logic-based image brightness correction and contrast adjustment method, followed by data normalization and block portioning scheme. The second contribution is a novel adaptive perturbation algorithm for designing a randomized, robust measurement matrix for image compression using a CS-based approach [33]. A two-level encryption scheme is formulated for securing compressed image data and reconstruction parameters. Compressed images are encrypted using proposed cross-pixel and intra-pixel permutation, while reconstruction parameters are encrypted using lightweight public-key encryption to ensure secure transmission in telemedicine. The novelty is in offering compression at sender side, secure transmission, and efficient reconstruction at receiver. A high security is ensured as each module is connected with others and highly sensitive to input parameters, makes it hard for unauthorized parties to foresee or reverse-engineer the compression sequences and protecting data from interception or tampering.

2. Method

This section discusses the methodology adopted and presents system implementation followed by mathematical modelling and algorithmic discussion. Firstly fuzzy-logic-based image enhancement and block partitioning scheme are detailed. The study discusses the proposed numerical algorithms for constructing a robust measurement matrix, a core part of CS-based compression. Afterwards, the numerical algorithms proposed for CS-based image compression, lightweight encryption and image reconstruction would be discussed to enable cost-effective and reliable medical data transmission in telemedicine.

Fuzzy-Logic-Based Contrast Adjustment

The medical images after acquisition often contain motion artifacts, random noise, and poor illumination, which may lead to loss of essential information during compression and encryption. Hence, the proposed study implements a fuzzy logic-based contrast adjustment method to improve image visual quality. The adoption of fuzzy logic provides a robust way for dealing with uncertainties and imprecise transitions while modifying pixel intensities to enhance contrast among image regions. The study takes single-channel intensity image of uniform size in height and width as its input and applies a fuzzy logic to enhance the contrast variables input pixel intensity and output contrast adjustment, as shown in Table 1.

Table 1: Highlights of proposed fuzzy logic variables

Input pixel intensity	Output contrast adjustment
Very Dark	Very Dark
Dark	Slightly Dark
Dark Gray	No Change
Gray	Slightly Bright
Light Gray	Very Bright
Bright	
Very Bright	

The input and output variable values are decided based on the fact that pixel values in a grayscale image, ranging from [0, 255], can be classified into different categories that represent Gaussian and trapezoidal membership functions, thereby enabling smooth transitions between intensity levels and capturing minor pixel intensity changes. Similarly, the output variable for contrast adjustment is divided into five fuzzy sets, defining how much each pixel should be adjusted. Therefore, a custom rule set is defined for image enhancement, as shown in Table 2.

Table 2: Adopted rule set in the fuzzy system

Rules	Description
Rule 1	The new pixel value should be slightly dark if the pixel intensity is very dark.
Rule 2	If the pixel intensity is dark gray, the new pixel value should be slightly dark.
Rule 3	If the pixel intensity is gray, the new pixel value should be slightly dark.
Rule 4	If the pixel intensity is bright, the new pixel value should be slightly bright.
Rule 5	If the pixel intensity is dark, the new pixel value should be very dark.
Rule 6	If the pixel intensity is very bright, the new pixel value should remain unchanged.

The rules in Table 2 enables the system to enhance image contrast adaptively depending on pixel properties or intensity levels without sudden changes. The fuzzy inference system is applied for every grayscale pixel, calculating its level of belonging to fuzzy sets and producing a new intensity value based on given rules. The output pixel values are clipped to remain within 0–255 and are stored to a new matrix. Additionally, a block segmentation strategy is employed to segmenting the enhanced image I_E into multiple disjoint blocks of size $(r \times c)$ where r denotes the row, and c is a column in each block. The implementation steps of block segmentation are described in the Algorithm-1. The study initializes an empty matrix B (Step 1) and then initializes predefined block dimensions r and c, so that the entire input image I_E is covered without overlap (Step 2).

Algorithm-1 Input image preprocessing

1. Initialize an empty matrix B of size $(n \times m)$ to store the image blocks.
2. Define block dimensions r and c such that $r \times n = M$ and $c \times m = N$
3. For each $i \in \{0,1,2,\cdots,n-1\}$ and $j \in \{0,1,2,\cdots,m-1\}$,
   Compute starting point of block: $x = i \times r$, $y = j \times c$
   Segment I_E to obtain blocks $B_{i,j}$:
   $B_{i,j} = I_E[x{:}\, x + r, y{:}\, y + c]$
4. Append $B_{i,j}$ to matrix B

For each block segment, the algorithm calculates the starting point of the blocks and extracts it from I_E as shown in (Step 3). The indexing for the block follows a row-wise order, where i iterates over the rows (height) and j iterates over the columns (width) of the image. This results in a partitioning of the I_E into n×m blocks, each with dimension $r \times c$. These blocks are then appended to the matrix B (Step 4). This block segmentation operation also enables parallel processing, which can be effective in scenarios with computational constraints, such as the telemedicine ecosystem.

Dynamic measurement matrix

Unlike existing works where 1D logistic maps were used in the CS-based approaches, the proposed study presents a numerical algorithm that adopts a pseudo-2D-logistic map optimized by a novel adaptive perturbation scheme to construct dynamic and pixel-adaptive measurement matrices for both compression and encryption. The proposed pseudo-2D-Logistic-Map as shown in Equ (1) is designed by integrating the logistic map with elements from the Henon map, numerically expressed as follows:

1) $x_{n+1} = r \times x_n(1 - x_n) + \alpha(\epsilon H(x_n, y_n))$

Where, $H(x_n, y_n)$, represents the Henon map's influence, ϵ is a small perturbation parameter, small perturbation parameter ϵ and α is a fixed scaling factor to control the influence of the Henon map on the logistic equation. The steps involved in formulation of pseudo-2D-Logistic-Map is discussed as follows:

The logistic map, a one-dimensional dynamic system as shown in Equ (2) described as follows:

2) $x_{n+1} = r \times x_n \times (1 - x_n)$

The Henon maps, a two-dimensional dynamic system in Equ (3) is described as below:

3) $x_{n+1} = 1 - a \times x_n^2 + y_n \;\; \& \;\; y_{n+1} = b \times x_n$

The proposed pseudo-2D-Logistic-Map is a complex dynamic system that draws from the characteristics of both maps as described in the above Equ (1). after direct modulation, the proposed pseudo-2D Logistic Map is expressed as Equation (4) :

4) $x_{n+1} = r \times x_n(1 - x_n) + \alpha\big(\epsilon H(x_n)\big) \; mod \; 1$

The inclusion of the mod 1 operation ensures that, regardless of how large the values become due to the addition of the logistic and Henon sequences, they are covered back into the [0, 1] interval. This effectively prevents overflow, keeping the values within the representable floating-point range. The implementation of the proposed Pseudo-2D-logistic map is described in Algorithm 2, which considers multiple inputs, such as one predefined initial condition x_0, dynamically assigned initial condition y_0 from algorithm-3, sequence length (n) and growth rate (r).

Algorithm-2 Pseudo-2D-logistic-sequence

Input: x_0,y_0, n, r

Output: L (logistic sequences with complex chaotic dynamics)

Start

1. Initialize constants a, b, α (α is the modulation factor for the Henon map's influence)
2. Initialize two arrays X and Y of length n
3. Set initial value $X[0] = x_0$ and $Y[0] = y_0$ to store 2D sequence values
4. For each index, i from 1 to n-1
5. Update $X[i]$ and $Y[i]$ according to Henon map equ (3)
   $X[i] = 1 - a \times (X[i-1])^2 + Y[i-1]$ & $Y[i] = b \times X[i-1]$
6. Initialize an array L of length for the logistic sequence
7. Set initial value $L[0] = x_0$
8. For each index, i from 1 to n-1
9. Compute $L[i]$ by integrating the logistic map's dynamics with the Henon sequence X and apply direct modulation operation: $L[i] = (r \times L[i-1] \times (1 - L[i-1]) + \alpha \times X[i-1]) \bmod 1$
10. Return L

End

After successful execution, it returns a logistic sequence L as its output. To make the generated logistic sequences more dynamic, the proposed study develops an adaptive perturbation scheme that introduces a unique mechanism for the dynamic adjustment of the initial condition y_0 in the proposed algorithm-2. This perturbation scheme dynamically selects the initial condition y_0 based on the edge density of the image blocks, which is decided based on the hypothesis that the edge density of an image block reflects its informational complexity and, consequently, its suitability initial conditions in the chaotic sequence generation process. Algorithm 3 describes the implementation procedure of the proposed adaptive perturbation scheme, where for each block a gradient magnitude $G_{x,y}$is computed using the Sobel operator that applies a pair of convolution kernels S_x and S_y of size 3x3 to the image blocks (Step 1-2).

Algorithm-3 Adaptive Perturbation Scheme

Input: B_i (image blocks obtained from the Algorithm-1)

Output: y_0

Start

1. For each image block B_i
2. Compute the gradient magnitudes. $G_{x,y} = \sqrt{(S_x \otimes B_i)^2 + (S_y \otimes B_i)^2}$, Where, S_x and S_y are Sobel kernels for horizontal and vertical edges, respectively, and $\otimes$ is a convolution operator.
3. Compute edge density: $E_d(B_i) = \frac{|\{(x,y)|G_{x,y} > \mu(G_{x,y})\}|}{N}$, Where, $\mu(G_{x,y})$ is mean gradient magnitude and N is the total number of pixels
4. Aggregate the edge densities $\{E_d(B_1), E_d(B_2), E_d(B_3), E_d(B_4)\}$
5. Sort edge density values in ascending order to prioritize blocks
6. **Utilize function** $f_2(E_d)$ to determine y_0, by mapping edge densities to initial conditions within the predefined intervals
7. If $E_d(B_i) \in [l_1, u_1)$, then $y_0 = \lfloor E_d(B_i), 4 \rceil$ // cut-off for lower range
8. $E_d(B_i) \in [l_2, u_2)$, then $y_0 = \lfloor E_d(B_i), 4 \rceil$ // cut-off for middle range
9. Otherwise, assign $y_0 = d$, where d is a default value ensuring a robust starting point for chaotic sequence generation.
10. Return output y_0

End

The next step of the algorithm computes edge density $E_d(B_i)$ for each pixel in image blocks, as the ratio of the number of pixels where the gradient magnitude exceeds the mean gradient magnitude $\mu(G_{x,y})$ to the total number of pixels N in the blocks (Step 3). In the subsequent steps, the obtained edge densities for all blocks are aggregated and then sorted in ascending order (Step 4-5) to prioritize image blocks based on their complexity and ensure that

initial conditions are adjusted in a manner that reflects the varying levels of detail across the image, enhancing the adaptiveness of the process. In the further steps (6-9) a selection function $f_2(.)$ is then employed over obtained values of E_d to map edge densities to initial conditions within predefined intervals, which are empirically determined based on a comprehensive analysis of how edge density correlates with image block's visual and optimal chaotic dynamics. This scheme ensures that essential details are preserved even at higher compression ratios by adapting initial conditions to image features.

Proposed CS-Based Compression

The procedure for image compression under a CS framework involves generating two distinct logistic sequences subsequently to form robust measurement matrices Φ. The first logistic sequence, L1, is generated using the function $f_2(\,)$ (algorithm-2) with parameters (x_0, y_0, n, r). In order to augment the Φ matrix robustness, a second sequence, L2, is derived by swapping the initial conditions as in Equ (5) and Equ (6).

5) $L1 = f_2(x_0, y_0, n, r)$

6) $L2 = f_2(y_0, x_0, n, r)$

7) $\Phi = \begin{cases} \Phi 1 & if\ i\%2 == 0 \\ \Phi 2 & if\ i\%2 \neq 0 \end{cases}$

The construction of Φ matrix subjected to a process where each row is a shifted version of the logistic sequence, scaled by a factor λ and sampling ratio sr. For a given logistic sequence L={L0,L1,⋯L(n-1) } and a scaling factor λ, the matrix Φ is constructed as described in Equ (7), where, Φ1=Ψ(L1,λ,sr), Φ2=Ψ(L2,λ, sr) and Ψ is a function that encapsulates the shifting and scaling operations. The procedure of image compression considers image blocks B_i, where each block is transformed into a frequency domain using DCT for enhancing the sparsity of the image chunks in the frequency domain as a prerequisite step for effective CS operation. Therefore, the DCT-transformed blocks D_i(u,v) represents the DCT coefficients at frequency coordinates (u,v), B_i(x,y) is the pixel value at spatial coordinates (x,y), α(u) and α(v) are normalization factors. The compression is achieved by projecting the DCT-transformed image chunks D_i onto the basis formed by the Φ matrix, such that:

8) $\mathbb{C}_i = \Phi \times D_i$

Where, Φ is the measurement matrix corresponding to Φ1 and Φ2, and D_i is the DCT coefficients and $\mathbb{C}_i$ represents the compressed blocks $\{\mathbb{C}_1, \mathbb{C}_2, \mathbb{C}_3, \mathbb{C}_4\}$ of the input image under CS approach. However, reconstruction of the compressed image to its original form at the receiver side requires the exact initial conditions and parameters used during compression, such as initial conditions (x_0, y_0), sequence length (n), and growth rate (r). But during transmission an attacker can intercept the compressed medical images and their associated parameters, which can lead to unauthorized access to sensitive medical data, potential manipulation of the data, and compromised data integrity. The next section describes the proposed encryption technique for secure transmission.

Lightweight Encryption

We propose a hybrid encryption mechanism that combines chaotic matrix cypher (CMC) operation and lightweight asymmetric encryption to ensure data integrity and speedy transmission in a distributed environment like telemedicine. The first layer uses CMC to encrypt the compressed data for confidentiality. The second layer utilizes a custom lightweight asymmetric encryption method to encrypt the critical parameters, which act as the secret key required to decrypt and reconstruct the data into its original form. The implementation of CMC is detailed in the Algorithm 4.

Algorithm-4 CMC Encryption

Input: Compressed image chucks $\mathbb{C} = \{\mathbb{C}_1, \mathbb{C}_2, \mathbb{C}_3, \mathbb{C}_4\}, \Phi\}$, and λ

Output: $\mathcal{E} = \{E_1, E_2, E_3, E_4\}$ encrypted image chunks

Start

1. For each $\Phi_i \in \Phi$, construct a transformation matrix, $\Theta_i = \frac{\Theta_i}{\lambda}$
2. Initialize $\mathcal{E} \leftarrow \mathbb{C}$ initially,
3. For each pair (E_i, E_{i+1}) in $\mathcal{E}$:

   Determine $\Theta = \Theta_{(i\ mod\ 2)+1}$

   For each pixel location (m, n) in E_i:

   Compute the transformation indices from matrix Θ as:

$$(\hat{m}, \hat{n}) = (\lfloor (N-1) \times sin(2\pi\Theta_{mn}) \rfloor,\ \lfloor (N-1) \times cos(2\pi\Theta_{mn}) \rfloor)$$

   Execute pixel permutation based on ′s relation to $\overline{\Theta}$ (mean value of Θ)

If $\Theta_{mn} > \bar{\Theta}$, do cross-pixel permutation:

$E_i(m,n), E_{i+1}(\hat{m},\hat{n}) \leftarrow E_{i+1}(\hat{m},\hat{n}), E_i(m,n)$

$E_i(m,n), E_{i+1}(m,n) \leftarrow E_{i+1}(m,n), E_i(m,n)$

else if $\Theta_{mn} \leq \bar{\Theta}$, do intra-pixel permutation:

$E_i(m,n), E_i(\hat{m},\hat{n}) \leftarrow E_i(\hat{m},\hat{n}), E_i(m,n)$

$E_{i+1}(m,n), E_{i+1}(\hat{m},\hat{n}) \leftarrow E_{i+1}(\hat{m},\hat{n}), E_{i+1}(m,n)$

4. Return $\mathcal{E}$ after iterating through all chunk pairs.

End

The proposed CMC algorithm takes inputs of compressed image blocks C, measurement matrices Φ, and a scaling factor λ. It produces a set of encrypted image blocks E=$\{E_1, E_2, E_3, E_4\}$ using non-linear transformations and pixel permutations. For each Φ a transformation matrix Θ_i is constructed by dividing $\Theta_i$by λ (Step-1), thereby ensuring chaotic properties are incorporated into the matrices. A placeholder E is initialized to C, which is updated during encryption (Step-2). The core encryption uses a matrix-driven pixel permutation scheme, iteratively applied for each block pair (E_i, E_{i+1}) of compressed blocks in E (step-3). Then matrix Θ is selected using modulo arithmetic to alternate between Φ_1 and Φ_2 and for each pixel's coordinates (m,n) in the current image block E_i, the algorithm determines the new transformation indexes or coordinates (m,n) using sine and cosine functions applied to the elements of transformation matrix Φ. This process introduces non-linearity and highly randomized behaviour into the index transformation. Afterwards, using the obtained transformation coordinates (m,n), the algorithm performs pixel permutations process considering the value of Θ_{mn} relative to its mean value $\bar{\Theta}$shown in Equ (9).

9) $$\bar{\Theta} \leftarrow \left\lfloor \frac{1}{m \times n} \sum_{i=1}^{m} \sum_{j=1}^{n} \Phi_{ij} \right\rfloor$$

The process of pixel permutations is a cross-pixel and intra-pixel permutation for achieving highly randomized encryption. The algorithm here checks the condition $\Theta_{mn}>\Theta$ to execute cross-pixel permutation; otherwise, it checks for $\Theta_{mn}\leq \bar{\Theta}$ to execute the intra-pixel permutation process. This step ensures that the pixel values are permuted in a highly complex and random manner to enhance the robustness of the encryption process. The similar pixel permutation processes repeat for all pairs of image chunks in an iterative manner, and after completion, they return the final set of encrypted image blocks E (step-4). We also introduce a lightweight public-key encryption method using three smaller prime numbers to generate modulus n, thereby enabling Chinese Remainder Theorem (CRT) based decryption to get reduction in the computational process. The receiver generates a key pair and shares the public key via a trusted channel. The sender encrypts image reconstruction parameters and transmits them with encrypted blocks. This scheme offers efficient security as the encrypted blocks cannot be reconstructed without the receiver's private key.

Reconstruction

Upon receiving the encrypted image blocks and reconstruction parameters, the receiver uses their private key to decrypt the parameters, and then executes Algorithm 4 in decryption mode (reverse of encryption). The pixel permutations are reversed, reconstructing the original compressed blocks. After decryption, reconstruction uses the smoothed L_0 (SL_0) signal approximation algorithm which solves under-determined linear systems in compressed sensing. Here, SL_0 aims to find the sparsest solution by minimizing the L_0 norm (number of non-zero entries) and since L_0 is non-convex and hard to minimize directly, SL_0 minimizes smooth approximations of the L_0 norm. The key idea is to approximate the L_0 norm of a signal s with a continuous function that can be efficiently minimized using standard optimization techniques. The sparse recovery problem shown in Equation (10) can be formulated as:

10) $$min_s \left|\left|s\right|\right|_0 subjected\ to\ \Phi x = S$$

The SL_0 uses a decreasing sequence of smoothing parameters σ, for L_0 approximation. Afterwards, each decrypted blocks D_i is in the DCT domain due to prior compression. DCT coefficients d_i^{dct} are used for sparse recovery via SL_0. The initial sparse signal s_i is estimated using the pseudoinverse Φ^+ of the measurement matrix applied to d_i^{dct}, numerically given as follows:

11) $$s_i^{(0)} = \Phi^+ \times d_i^{dct}$$

The obtained signal $s_i^{(0)}$from Equ (11) is further refined over several iterations to enhance sparsity iteratively. The recovered sparse coefficients s_i are then transformed back into pixel values using the inverse DCT to reconstruct the image blocks in their original form. The individual blocks are then combined to form a complete image. The next section discusses the proposed system performance and outcome analysis.

3. Results And Discussion

The development of the proposed system is done using Python on a Windows 11 64-bit system. The performance analysis of the proposed system was carried out considering both visual and numerical analysis considering different useful statistical performance metrics. The proposed system was evaluated extensively to justify its effectiveness for the real-time telemedicine application. The study considers brain MRI images as high dimensional medical image from BraTS 2019, Br35H and MRBrainS13 databases.

Visual Analysis

The visual outcome in Figure 1, reveals the better image quality by the proposed fuzzy-logic based enhancement. The performance of the proposed system was quantitatively evaluated using the Peak Signal-to-Noise Ratio (PSNR) measured in decibels (dB). The formula for computing PSNR shown in Equ (12) is given as follows:

12) $$PSNR = 20 \times log_{10}\left(\frac{255}{\sqrt{MSE}}\right)$$

Where MSE is the mean square error, a critical indicator where preserving the reliability of medical images post-compression is important. This performance metric is utilized to measure the noise level introduced during the compression and encryption process, with values over 35 indicating superior image quality. Figure 2 and Figure 3 shows performance analysis concerning PSNR and SSIM metrics.

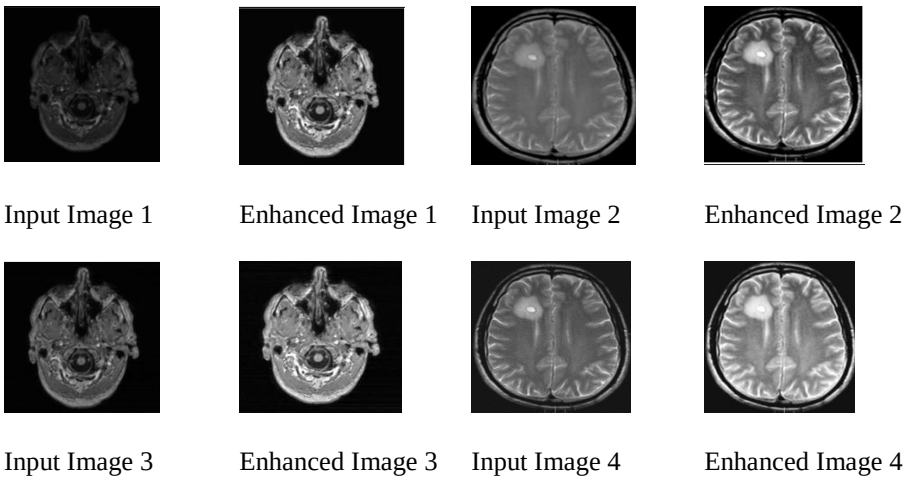

Figure 1. Presents visual outcome of the proposed Fuzzy logic-based image enhancement

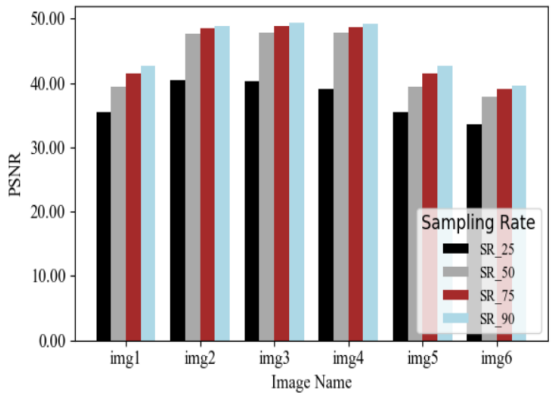

Figure 2. Shows PSNR analysis with varying sampling rates

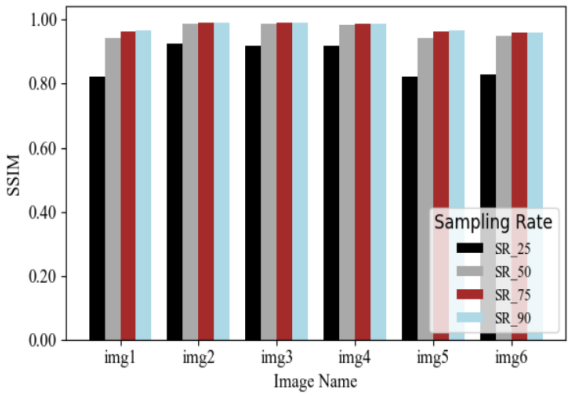

Figure 3. Shows SSIM analysis with varying sampling rates

Figure 2 presents a PSNR analysis for nine different input images of size 512x512 at four sampling rates. The outcome shows that PSNR values for all images remain above 35 dB across all sampling rates, indicating good reconstruction quality. The next analysis in Figure 3 was carried out regarding the Structural Similarity Index Measure (SSIM), which is a statistical approach to measure the similarity between two images as in Equ (13). The formula for SSIM is given as follows:

$$13) \qquad SSIM(x,y) = \frac{(2\mu_x\mu_y+c_1)(2\sigma_{xy}+c_2)}{(\mu_x^2+\mu_y^2+c_1)(\sigma_x^2+\sigma_y^2+c_1)}$$

Where, μ_x and μ_y are the average pixel intensities of images x and y, respectively. The next attribute σ_x^2 and σ_y^2 are the variances of pixel intensities of images, whereas σ_{xy} is the covariance of pixel intensities between image pixels and c_1 and c_2 are constants to stabilize the division with a weak denominator. The SSIM with values closer to 1 indicates higher similarity and, thus, better quality. The analysis of Figure 3 reveals that higher sampling rates generally result in higher SSIM values, indicating better reconstruction quality. The next analysis is carried out in terms of Cross Correlation (CC), expressed as shown in Equ (14), showing the preservation of linear characteristics:

$$14) \qquad CC = \frac{\sum_{i=1}^{n}(X_i-\bar{X})(Y_i-\bar{Y})}{\sqrt{\sum_{i=1}^{n}(X_i-\bar{X})^2\sum_{i=1}^{n}(Y_i-\bar{Y})^2}}$$

Where, n is the number of pairs of scores, X_i and Y_i are the values of the X and Y variables for the i-th pair and $\bar{X}$ is the mean of the X values, and $\bar{Y}$ is the mean of the Y values. Here, CC value close to 1 indicates a high degree of similarity. The performance assessment shown in Figure 4 towards CC for different images (512×512) at different sampling rates. It can be seen that the proposed system exhibits a strong positive trend with CC scores consistently exceed 0.98 in the first few cases, and approaching 1.0 at SR 50, 75, and 90. This signifies near-perfect reconstruction quality for these images. The next Figure 5 presents the processing times analysis for both the sender (encoding) and receiver (decoding). The performance of the proposed hybrid compressed sensing and encryption system was quantitatively evaluated by analyzing the processing time for both sender and receiver components considering different file sizes ranging from 10 to 100 MB. The analysis shows that the proposed system shows consistent linear processing time for different file sizes for both sender and receiver operations, which indicates the efficiency of the proposed system to handle different data volumes.

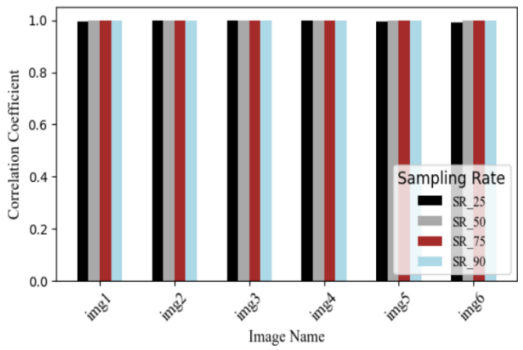

Figure 4. Shows CC analysis

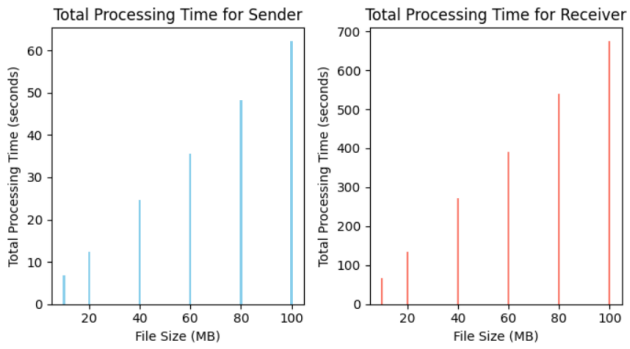

Figure 5. Presents processing time analysis

Comparative Analysis

In this section, we compare our proposed system with our previous work based on a neural network to compress the non-ROI areas of the image [26] and to compress ROI it adopted integer-based lifting wavelet transform for the ROI. This transform provided lossless compression, ensuring no critical information was lost during the compression process. Our previous approach [26] aimed to reduce the data's dimensionality and achieve high compression ratios. However, the neural network required significant computational resources, thereby increased processing times. Therefore, the comparison is done in Figure 6 considering PSNR, SSIM, and overall processing times for 512×512 image size and different sampling ratio (SR).

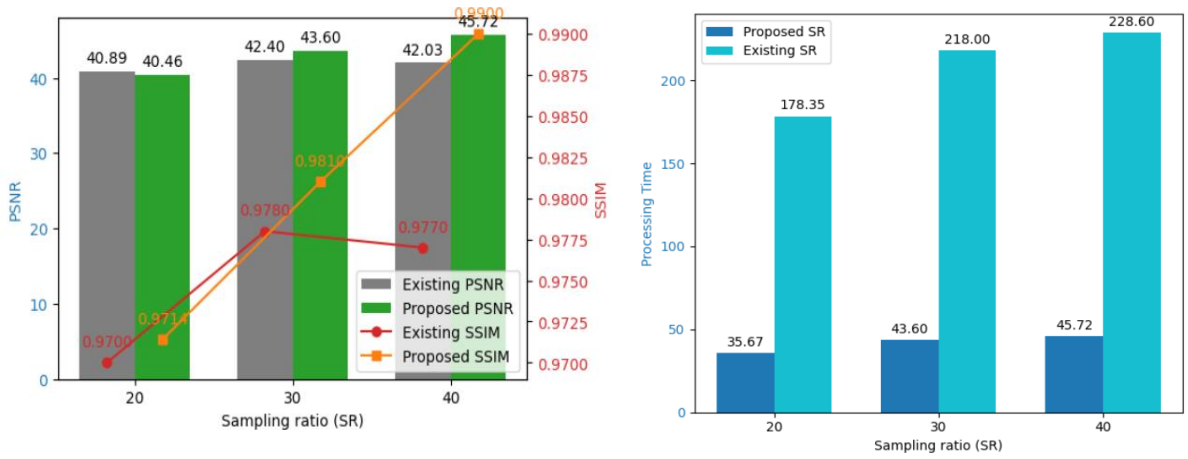

a) Analysis of the PSNR and SSIM

b) Analysis of processing time

Figure 6. Presents comparative assessment where a) presents analysis regarding PSNR and SSIM and b) shows processing time analysis of the proposed algorithm

Figure 6 (a) reveals that the proposed system outperforms our previous [26] compression scheme in terms of both PSNR and SSIM values at SR 30 and SR 40. At SR 20, while the existing system shows a slightly higher PSNR, the proposed system has a marginally better SSIM. This indicates that the proposed system maintains or improves image quality and structural similarity across different sampling rates. The above Figure 6 (b) shows a comparative analysis in terms of the overall processing time of the algorithm for image size 512x512 at different sampling rates. It can be seen that the proposed system takes very little time in the overall process from compression to reconstruction. On the other hand, our previous system takes an extensive processing time for compression and decryption due to neural networks and complex compression algorithms, resulting in significantly higher processing times.

Findings and Discussion

The proposed study addresses the critical requirements for secure and cost-effective transmission of high-quality medical image in telemedicine context by integrating proposed CS based compression and encryption in an highly synchronized manner. The comprehensive demonstrates that the hybrid compressed sensing and encryption system significantly enhances processing and security in telemedicine applications. Experimental analysis shows high PSNR across different SRs, though values vary by image due to differences in texture, contrast, and color distribution. SSIM analysis shows higher values at SR 75 and 90 compared to SR 25 and 50. The system achieves better reconstruction for low- and medium-quality images at SR 50, 75, and 90. In terms of processing time, the proposed algorithm showed stable performance with respect to different image sizes. In terms of processing time, the proposed algorithm showed stable performance with respect to different image sizes. The processing time for encoding is consistently faster than decoding, showing higher efficiency at the sender side. The lightweight public-key encryption significantly reduces encryption/decryption time, supporting real-time use. Furthermore, the adaptability of the proposed system is demonstrated through the dynamic adjustment of the chaotic sequence generation, which is finely adjusted to the specific image characteristics, which not only improves the robustness of the compression process but also enhances the overall security of the transmitted data. Although the proposed system improves both compression efficiency and security, it maintains balance with our earlier neural network-based system, which was more focused on strong compression capabilities but at the cost of substantial computational resources. The choice between systems should depend on whether the priority is storage efficiency or speed and security. Our future enhancements will explore reducing decoding time and expanding applicability to other medical data types needing secure, efficient transmission protocols.

4. Conclusion

This paper has presented a hybrid compressed sensing framework to enhance the safety and efficiency of MRI data transmission within the telemedicine ecosystem. The contributions of the proposed study are multiple. First, the proposed study has presented a multi-level preprocessing scheme to enhance image quality and reduce the computation demands in the compression and reconstruction phase. We then propose a novel numerical method, as described in Algorithms 2 and 3, which exploits the complexity of the input image and the unpredictability of chaos theory to provide a highly adaptive measurement matrix to prevent unauthorized access. In addition, this study introduced a two-layer encryption strategy to protect the security of compressed data and reconstruction

parameters when they are transmitted over telemedicine networks. A smooth L0 algorithm has been implemented for signal recovery to reconstruct high-quality images from compressed data. The work offers a highly synchronized and integrated approach to offer comprehensive security layers and efficient medical data transmission. Future work can be extended towards implementing self-adaptive techniques (such as reinforcement learning) that can dynamically adjust to different medical imaging modalities' different quality and feature requirements. In addition, the proposed work can be extended to incorporate blockchain technology for secure authorization and authentication.

References

[1] B Klaassen, B. J. van Beijnum, and H. J. Hermens, "Usability in telemedicine systems—A literature survey," *International Journal of Medical Informatics*, vol. 93, pp. 57-69, 2016.

[2] M. Pikkemaat, H. Thulesius, and V. Milos Nymberg, "Swedish primary care physicians' intentions to use telemedicine: A survey using a new questionnaire–physician attitudes and intentions to use telemedicine (pait)," International Journal of General Medicine, pp. 3445-3455, 2021.

[3] A. Elawady, A. Khalil, O. Assaf, S. Toure, and C. Cassidy, "Telemedicine during COVID-19: a survey of Health Care Professionals' perceptions," *Monaldi Archives for Chest Disease*, vol. 90, no. 4, 2020.

[4] C. O. Alenoghena, H. O. Ohize, A. O. Adejo, A. J. Onumanyi, E. E. Ohihoin, A. I. Balarabe, and B. Alenoghena, "Telemedicine: A survey of telecommunication technologies, developments, and challenges," *Journal of Sensor and Actuator Networks*, vol. 12, no. 2, p. 20, 2023.

[5] V. K. Bairagi, "Big data analytics in telemedicine: a role of medical image compression," *Big Data Management*, pp. 123-160, 2017.

[6] R. Thanki and S. Borra, "Medical Imaging and Its Security in Telemedicine Applications" Berlin/Heidelberg, Germany: *Springer International Publishing*, 2019.

[7] M. Magdy, K. M. Hosny, N. I. Ghali, and S. Ghoniemy, "Security of medical images for telemedicine: a systematic review," *Multimedia Tools and Applications*, vol. 81, no. 18, pp. 25101-25145, 2022.

[8] G. Vallathan and K. Jayanthi, "An integrated and secured medical data framework for effective tele health applications," *International Journal of Advanced Intelligence Paradigms*, vol. 18, no. 1, pp. 63-78, 2021.

[9] V. Anusuya, V. S. Raghavan, and G. Kavitha, "Lossless compression on MRI images using SWT," *Journal of Digital Imaging*, vol. 27, pp. 594-600, 2014.

[10] R. Sheeja and J. Sutha, "Soft fuzzy computing to medical image compression in wireless sensor network-based tele medicine system," *Multimedia Tools and Applications*, vol. 79, no. 15-16, pp. 10215-10232, 2020.

[11] M. Kaur and V. Wasson, "ROI based medical image compression for telemedicine application," *Procedia Computer Science*, vol. 70, pp. 579-585, 2015.

[12] S. N. Kumar, A. L. Fred, and P. S. Varghese, "Compression of CT images using contextual vector quantization with simulated annealing for telemedicine application," *Journal of Medical Systems*, vol. 42, no. 11, p. 218, 2018.

[13] M. Raeiatibanadkooki, S. R. Quchani, and M. KhalilZade, "Compression and encryption of ECG signal using wavelet and chaotically Huffman code in telemedicine application," *Journal of Medical Systems*, vol. 40, p. 73, 2016.

[14] K. M. Ameen Suhail and S. Sankar, "Image compression and encryption combining autoencoder and chaotic logistic map," *Iran. J. Sci. Technol. Trans. A Sci.*, vol. 44, no. 4, pp. 1091-1100, 2020, doi: 10.1007/s40995-020-00905-4.

[15] N. Baranwal, K. N. Singh, and A. K. Singh, "YOLO-based ROI selection for joint encryption and compression of medical images with reconstruction through super-resolution network," *Future Generation Computer Systems*, vol. 150, pp. 1-9, 2024.

[16] I. D. Irawati, S. Hadiyoso, and Y. S. Hariyani, "Multi-wavelet level comparison on compressive sensing for MRI image reconstruction," *Bull. Electr. Eng. Informatics*, vol. 9, no. 4, pp. 1461–1467, 2020, doi: 10.11591/eei.v9i4.2347.

[17] O. N. Aspan, R. Fleysher, and M. L. Lipton, "Compressed sensing MRI: a review of the clinical

literature," *The British journal of radiology*, vol. 88, 1056, doi: https://doi.org/10.1259/bjr.20150487.

[18] N. Zhou, H. Li, D. Wang, S. Pan, and Z. Zhou, "Image compression and encryption scheme based on 2D compressive sensing and fractional Mellin transform," Optics Communications, vol. 343, pp. 10-21, 2015.

[19] X. Chai, H. Wu, Z. Gan, Y. Zhang, Y. Chen, and K. W. Nixon, "An efficient visually meaningful image compression and encryption scheme based on compressive sensing and dynamic LSB embedding," *Optics and Lasers in Engineering*, vol. 124, p. 105837, 2020.

[20] A. Hadj Brahim, A. Ali Pacha, and N. Hadj Said, "Image encryption based on compressive sensing and chaos systems," Opt. Laser Technol., vol. 132, p. 106489, 2020, doi: 10.1016/j.optlastec.2020.106489.

[21] M. Lakshminarayana and M. Sarvagya, "MICCS: A novel framework for medical image compression using compressive sensing," *International Journal of Electrical and Computer Engineering (IJECE)*, vol. 8, no. 5, pp. 2818-2828, 2018.

[22] S. Zhu, C. Zhu, and W. Wang, "A Novel Image Compression-Encryption Scheme Based on Chaos and Compression Sensing," IEEE Access, vol. 6, pp. 67095-67107, 2018, doi: 10.1109/ACCESS.2018.2874336.

[23] T. M. Quan, T. Nguyen-Duc, and W.-K. Jeong, "Compressed Sensing MRI Reconstruction Using a Generative Adversarial Network With a Cyclic Loss," *IEEE Transactions on Medical Imaging*, vol. 37, no. 6, pp. 1488-1497, June 2018, doi: 10.1109/TMI.2018.2820120.

[24] R. Monika and S. Dhanalakshmi, "An efficient medical image compression technique for telemedicine systems," *Biomedical Signal Processing and Control*, vol. 80, p. 104404, 2023.

[25] C. V. Vivekanand, T. M. Inbamalar, K. P. Nadar, V. Kannagi, and P. Arthi Devarani, "Energy-Efficient Compressed Sensing in Cognitive Radio Network for Telemedicine Services," *Wireless Communications and Mobile Computing*, 2023.

[26] M. D. Deepak, P. Karthik, S. K. S, and H. C. Ravikumar, "Reconstruction of MR Images using Sparse Signal Sequences in Frequency Domain," *Int. J. Innov. Technol. Explor. Eng.*, vol. 9, no. 3, pp. 895–902, 2020, doi: 10.35940/ijitee.b7885.019320.

[27] Singh, S., Sood, V. and Sharma, B, "Systematic survey of compression algorithms in medical imaging." *In Advances in Computational Techniques for Biomedical Image Analysis*, pp. 205-230, 2020.

[28] Bourai, N.E.H., Merouani, H.F. & Djebbar, A. "Deep learning-assisted medical image compression challenges and opportunities: systematic review". *Neural Comput & Applic* 36, 10067–10108, 2024.

[29] S. M. Belgaonkar and V. Singh, "Image Compression and Reconstruction in Compressive Sensing Paradigm," *Glob. Transitions Proc., vol. 3*, no. April, pp. 220–224, 2022, doi: 10.1016/j.gltp.2022.03.026.

[30] P. Deora, B. Vasudeva, S. Bhattacharya, and P. M. Pradhan, "Structure preserving compressive sensing mri reconstruction using generative adversarial networks," *IEEE Comput. Soc. Conf. Comput. Vis. Pattern Recognit. Work.*, vol. 2020.

[31] S. Ravishankar, J. C. Ye, and J. A. Fessler, "Image Reconstruction: From Sparsity to Data-Adaptive Methods and Machine Learning," *Proc. IEEE*, vol. 108, no. 1, pp. 86–109, 2020,

[32] M. Mardani et al., "Deep generative adversarial neural networks for compressive sensing MRI," *IEEE Trans. Med. Imaging*, vol. 38, no. 1, pp. 167–179, 2019.

[33] Huimin Yu, Xuanwei Zhang,"Compressed sensing measurement matrix construction method based on uniform chaotic sequence and matrix factorization", *Measurement*,Volume 242, Part B,2025.